Journal of Marine Science and Engineering

Article

Methodological Aspects of Assessing the Thermal Load on Diesel Engine Parts for Operation on Alternative Fuel

Sergejus Lebedevas and Edmonas Milašius *

Faculty of Marine Technology and Natural Sciences, Klaipeda University, 91225 Klaipeda, Lithuania; sergejus.lebedevas@ku.lt
* Correspondence: edmonas.m@protonmail.com; Tel.: +370-60117362

Abstract: The decarbonization of maritime transport has become a crucial strategy for the adoption of renewable low-carbon fuels (LCFs) (MARPOL 73/78 (Annex VI) and COM (2021) 562-final 2021/0210 (COD)). In 2018, 98% of operated marine diesel engines ran on fossil fuels. The application of LCFs, according to expert assessments (DNV GL), is considered the most effective solution to the decarbonization challenge in the maritime sector. This publication presents methodological proposals related to assessing the reliability of operational diesel engines when transitioning to low- carbon fuels. The proposed methodology implements an interconnected assessment of the combustion cycle parameters and the limiting reliability factors of the thermal load on the most critical components of the cylinder–piston group. The optimization of the combustion cycle parameters for the indicators of energy and the environmental efficiency of low-carbon fuel applications was combined with the evaluation and assurance of permissible values of the thermal load factors on the components to determine the overall reliability of the engine. Thus, the possibility of overload and engine failures was already eliminated at the retrofitting design stage. The algorithm for the parametric analysis was grounded in the practical application of established α-formulae for the heat exchange intensity, such as those of the Central Diesel Engine Research Institute and G. Woschni. This approach was combined with modeling the combustion cycle parameters by employing statistical or single-zone mathematical models such as IMPULS and AVL BOOST. The α-formulae for low carbon fuels were verified based on the thermal balance data. The structure of the solutions for the effectiveness of the practical implementation of this methodology was comprehensively oriented towards diesel "families", as exemplified by the models 15/15 (p_{mi} = 1.2, 1.4, and 1.6 MPa). The long-term goal of the obtained results in the structure of comprehensive decarbonization research was to assess the factors of the reliable operation of characteristic groups of medium-speed (350–1000 rpm) and high-speed (1000–2100 rpm) marine engines for reliable operation in the medium term on ammonia.

Keywords: decarbonization of operational diesel fleet; combustion cycle; mechanical and thermal load factors; parametric analysis

check for updates

Citation: Lebedevas, S.; Milašius, E. Methodological Aspects of Assessing the Thermal Load on Diesel Engine Parts for Operation on Alternative Fuel. *J. Mar. Sci. Eng.* **2024**, *12*, 325. https://doi.org/10.3390/jmse12020325

Academic Editors: Jian Wu, Xianhua Wu and Lang Xu

Received: 21 December 2023
Revised: 8 February 2024
Accepted: 11 February 2024
Published: 13 February 2024

Correction Statement: This article has been republished with a minor change. The change does not affect the scientific content of the article and further details are available within the backmatter of the website version of this article.

1. Introduction

The most important direction for the development of maritime shipping is decarbonization and increasing the energy efficiency of marine diesel engines. Strategic plans for decarbonization are defined in the regulations of the International Maritime Organization, MARPOL 73/78 (Annex VI) [1]; the European Parliament and the Council, COM (2021) 562-final 2021/0210 (COD) [2] COM (2021) 559-final 2021/0223 (COD) [3]; and many others.

The maritime transport sector was the first sector globally to implement greenhouse gas (GHG) emission monitoring; additionally, it boasts reduction factors regulated in the form of environmental normative indices, both for newly built ships and, as of 2023, for entire operating fleets [1]. The energy efficiency design index, mandatory for all newly built ships, was introduced on 1 January 2013. The CO_2 reduction level of the first stage (grams of CO_2 per ton of cargo per nautical mile) was set at 10% below the baseline, and it will be progressively increased to achieve a 40% reduction by 2030 compared with the reduction levels of 2008 [1,4]. The suggestions for achieving the desired energy efficiency and decarbonization level include reducing the resistance of the ship hull, using waste heat recovery systems, increasing the energy efficiency of auxiliary power units, and using low-carbon fuels (LCFs) [1,5]. Recent legislation for reducing GHG emissions has considered reducing the CH_4 and N_2O levels, in addition to the CO_2 levels, as they are up to 50 and 250 times more harmful, respectively, to the ozone layer compared with CO_2 [2]. The energy efficiency existing ship index and the annual operation carbon intensity indicator were introduced on 1 January 2023, with the aim of giving ratings as soon as 2024. For ships in service, the energy efficiency can be improved by optimizing the propellers, reducing the speed by limiting the engine power, and implementing technological systems for the regeneration of alternative energy sources: utilizing wind energy (parachutes and Magnus-effect devices) while gradually transitioning to LCFs [5]. Experts consider using LCFs to be the most effective strategy for achieving decarbonization goals, with its benefits estimated at 20–22% [5] according to the classification society DNV GL, whereas other measures offer, on average, only a 4–7% improvement [5].

The attractiveness of using LCFs is determined by the technological features of the internal combustion engine (ICE) of the ship, unlike other types of transport. According to the IMO's fourth GHG study [6], 98.4% of all engines used in the fleet in 2018 were conventional fuel-oil engines; therefore, to achieve the decarbonization targets set for the transition period of 2030–2035, the use of LCFs, such as biofuels and liquefied natural gas (LNG), is one of the options, which can be later gradually switched to bio-LNG, ammonia, e-diesel, and other LCFs [2,5].

According to LR/UMAS (2020) [7], maritime infrastructure is ready for second- and third-generation biodiesel, e-diesel, bio-LNG, and e-LNG. However, the price of such fuel is significantly higher compared with that of fossil fuels [8]; according to 2020 data, the prices of e-diesel, biodiesel, and bio-LNG are 1280%, 260–400%, and 500% higher compared with that of fossil fuels, respectively. The use of methanol on ships is in the initial stage of practical solutions [2,5], and ammonia and hydrogen are in the stage of pilot technological solutions [5,7]. Since LNG is a fossil fuel with a lower CO_2 emission factor per kg of fuel, LNG is considered a transition fuel in the short term (until 2030). Major marine engine manufacturers such as MAN and Wartsila have developed and produced a range of dual-fuel (DF) engines that run on both diesel and LNG, with power outputs of up to 20,700 kW [9]. These engines are optimized to run on LNG and diesel, and their engine resources are guaranteed by the manufacturer. Simultaneously, the use of LNG in ships already in service has been widely studied, primarily in terms of engine energy efficiency [10,11], environmental aspects [12], and economic aspects [13,14].

However, research on engine reliability when transitioning to LCFs is lacking. The major research question in this aspect is whether the changes in mechanical and thermal stresses are at acceptable levels.

Research on decarbonization and engine reliability when transitioning from diesel-based to LCF-based engines has begun at Klaipeda University, and it includes developing main and auxiliary engines in the Lithuanian fleet; in the initial stage, basic methodological solutions and tool formats for their practical implementation are being considered.

This study provides a methodological basis for implementing interrelated solutions for optimizing the combustion cycle parameters and the mechanical and element thermal stress factors when operating engines on LCFs. This method is intended for implementation in low-, medium-, and high-speed marine engine groups operating mainly on biodiesel and LNG (bio-LNG); it is expected to cover the use of ammonia.

Factors Influencing Thermal Loading of Engine Parts and Their Impact on Reliability

The reliability of an ICE is determined by several interrelated factors: the design and material properties of the components, or sub-assemblies, and the mechanical and thermal loading factors that form the temperature and stress field [15,16]. To convert engines to LCF operation, due to limited retrofitting capabilities, changes in the design and materials are assumed to not be foreseen. In the cylinder–piston group (CPG) parts, which experience the most stress and limit the engine reliability factor, the thermal stresses amount to more than 50% [17], and up to 90% in the old-generation engine models. Therefore, to ensure that the mechanical stress level designed by the CPG is not exceeded during retrofitting (engine operation with LCFs), the maximum cycle pressure (P_{max}), the main influencing factor, was assumed as a constant. Thus, engine reliability for LCF operation can be ensured by assessing the thermal stresses; further, the thermal stresses can be kept under permissible levels by optimizing the characteristic parameters of the combustion cycle. When retrofitting an engine for LCF, significant attention is given to monitoring and ensuring the effective operation of the engine cooling system. The alteration of heat dissipation in the cylinder during LCF combustion should not lead to the engine overheating due to an insufficient thermal performance of the cooling system. This aspect, along with the optimization of the LCF combustion cycle, is increasingly attracting the attention of researchers. To avoid catastrophic failures, it is assumed that a well-designed cooling system, capable of handling the engine's nominal power on diesel fuel over extended periods, is in place. For example, Cabuk A.S.'s [18] study focuses on using IoT technology to minimize maintenance costs and prevent failures in ship cooling systems. The system integrates smart sensors and Node-Red, allowing remote monitoring of ship engines and cooling pumps. It detects and analyzes real-time data, providing valuable insights into current, temperature, and vibration to ensure the effective operation of the system. Since most marine cooling pumps are currently centrifugal, and ongoing studies are exploring alternative, more efficient solutions. To ensure adequate performance reserves in the cooling system and thereby avoid overload, Fatigati et al. [19] explore and optimize a Low-Speed Sliding Vane Rotary Pump (LS SVRP) used in internal combustion engine cooling. Employing a model-based design approach, the research reduces revolution speed to enhance volumetric capability without increasing pump dimensions significantly. The LS SVRP prototype, tested across various conditions, achieves overall efficiencies nearing 60%, surpassing centrifugal pumps, and the SVRP demonstrates an efficiency much less dependent on operating conditions. Another study by Di Giovine et. al. [20] introduces a lumped parameter model for a triple-screw pump, experimentally validated to explore its potential as an efficient alternative to centrifugal pumps in internal combustion engine-cooling circuits. The model achieves a mean error of 0.6% in flow rate calculations and demonstrates satisfactory volumetric efficiency compared to experimental data. Mechanical efficiency calculations, influenced by variable friction coefficients, yield a global efficiency of up to 70%. The model is applied to estimate the efficiency of a triple-screw pump as a cooling pump for an F1C IVECO 3l engine, showing an 8% improvement over a standard centrifugal pump. This aspect of retrofitting the cooling system should also be carefully considered as a means of ensuring acceptable thermal loads on the components of a diesel engine during its operation on LCF, thereby enhancing overall efficiency.

On the other hand, the thermal load on a part is characterized by the maximum temperature according to the material properties, the limiting temperature in the characteristic zones of the part (e.g., in the area of the upper compression ring of the piston), and the thermal stresses. For the CPG parts of ICEs, the thermal load (without changing the structure or boundary conditions of heat dissipation from the part) is determined by the coefficient of heat release from the working body (α_{gas}) and the temperature (T_{gas}). The existing analytical descriptions of α_{gas}, which determines the heat transfer intensity, can be divided into two groups of simplified mathematical models: those based on similarity theory criteria, and those based on the classical theoretical foundations of extended gas dynamics. Among these, the simplified mathematical models (MMs) of the first group are the most widely used models. The analytical solutions by Woschni 1967 [21], Hohenberg 1979 [22], Annand 1963 [23], Sitkei 1972 [24], Chang 2004 [25], Wu 2009 [26], and others operate with relatively easy-to-determine combustion cycle parameters. Typically, the classical criteria of the similarity theory of heat transfer (Nusselt number (Nu), Reynolds number

(Re), and Prandtl (Pr)) are used as the analytical basis for formulating αgas formulae; the constants in the formulae are determined from statistical summaries of the experimental data. These formulae are widely applicable owing to the statistical generalizations of the experimental data for different types of engines and the accuracy of the obtained results. Recently, classical α_{gas} solutions have been modified based on the results of a limited experiment or MM of a single-engine model [21–23], including an engine running on LCFs.

For example, Rabeti et al. [27] investigated the heat transfer coefficient of a homogeneous charge compression ignition engine running on natural gas. The study determined the errors in the heat transfer coefficient calculations and compared them to the 3D model results using calibrated coefficients from classical MMs. A single-cylinder Waukesha engine (82.55/114.3) at 800/1100/1400 rpm and with different inlet pressures was used for the tests. The heat transfer coefficient calculations were performed using a zero-dimensional, single-zone model to compare the accuracy of the MM, as no experimental studies were available at that time to verify the baseline. A 3D computational fluid dynamics (CFD) model with detailed chemical kinetics simulation results was used for verification. In turn, the reliability of the 3D model simulation was verified by calculating the heat transfer coefficient when the engine was running on petrol and comparing it with the experimental data. Several operating modes were simulated with varying engine speeds and intake pressures. The results showed that single-zone MMs overestimated the heat release coefficients compared with the 3D model using natural gas and standard coefficients, and calibrated α_{gas} scaling coefficients were recommended. With calibrated scaling coefficients, the closest results were obtained by Assanis [25] and Hohenberg [22], with average errors of 14.3% and 16.3%, respectively. Moreover, an evaluation of the solutions of [27] revealed that single-zone MMs are sensitive to the fuel type and combustion characteristics.

Depcik et al. [28] evaluated the possibility of applying classical heat transfer coefficient calculation models to small-displacement ICEs. Small ICEs of <100 cm^3 have a combustion chamber with a relatively large external surface area; this directly affects the heat loss to the cylinder wall and reduces the overall energy efficiency. Therefore, using conventional heat transfer correlations, their study attempted to adapt the α_{gas} calculations developed for larger engines to the study subject, which was a 3W-55i (44/35) engine with a power output of 4.4 kW and a maximum speed of 8500 min^{-1}. The results confirmed the applicability of the calculations of large-ICE heat transfer coefficients to small engines with parameter optimization.

Hassan et al. [29] investigated the applicability of heat transfer coefficients using the Woschni [21] equations for an engine running on gasoline fuel; 1D and 3D MMs were used. With a four-stroke, single-cylinder, 114.8 cm^3, high-speed, 1500–9500 min^{-1} motorcycle engine as the study subject, they investigated the temperature conditions of the intake and exhaust valves and the heat balance of the engine. The valve temperatures were measured using thermocouples and compared with the simulation data. Reportedly, the temperature errors at the intake and exhaust valves were 3.73% and 0.17% at 2500 min^{-1} and 4.12% and 0.70% at 5500 min^{-1}, respectively. The highest temperature regions were concentrated around the combustion surface, the highest heat flow was transmitted through the exhaust valve, the highest temperature was recorded at the exhaust valve neck, and the highest temperature of the intake valve was recorded at the combustion surface. Through these studies, the MM was determined, and the engine heat balance and thermal stresses were experimentally verified.

In summary, the applicability of α_{gas} MMs developed based on the classical similarity theory has been confirmed in new-generation ICEs of different sizes and purposes. In the absence of new proposals for analytical α_{gas} solutions, classical α_{gas} MMs are widely used to solve practical problems. However, their practical testing is limited in the case of LCFs, which makes research in this area relevant and in demand when solving problems involving the decarbonization of transport.

The second group of α_{gas} MMs is based on the classical theoretical foundations of extended gas dynamics after applying them to the physical processes in the ICE cylinder during the combustion cycle. Petrichenko [30] proposed such an MM, as follows:

$$\frac{\partial p}{\partial t} + \text{div}\ \rho_v = 0;\ \begin{cases} \rho\left(\frac{\partial v_i}{\partial x} + v_{i,j}v_i\right) = -\frac{1}{H_i}\frac{\partial p}{\partial q_i} + \tau_{ij,j}; \\ \rho c_p\left(\frac{\partial T}{\partial t} + \frac{v_j}{H_j}\frac{\partial T}{\partial q_j}\right) + div\ q = q_{v.} \end{cases}, \tag{1}$$

where ρ is the density; t is the time; v is the fluid motion vector with component ν_i (i = 1, 2, 3); H_i is the corresponding metric coefficient (Lamé coefficients); $\nu_{i,j}$ is the absolute derivative of component ν_i in coordinate q_j; p is the pressure; T is the temperature; $-\tau_{ij,j}$ is the absolute derivative of the tangent friction tensor in coordinate q_j; c_p is the specific heat capacity of fluids; q is the heat flow density vector; and q_v is the volumetric density of internal heat.

However, the practical application of these models, particularly for diesel engines in operation, is challenging because they are based on numerous differential equation variables, so they require extensive research under laboratory conditions and detailed graphical material of the design geometry. This type of analytical solution is partially used exclusively in multizone combustion cycle study models, such as AVL Fire and KIVA-3V [31,32].

Taking a closer look at the application of LCFs to an already operational fleet of ship engines, two main directions of scientific research emerge. The primary focus lies in researching and optimizing energy efficiency and environmental indicators. Another ongoing area of research pertains to the economic aspects of the operational fleet's transition to low-carbon fuels. Typically, addressing the failures of engine components identified during operation involves changing the materials, optimizing the construction, and employing detailed temperature field modeling for heat transfer coefficients while operating with traditional petroleum-derived fuels. The authors propose a methodological solution that combines a variation optimization stage for engine operation with low-carbon fuels and simultaneously evaluates the factors most affecting the reliability of the most thermally loaded components, such as pistons. Such solution principles were not found in the available literature.

For the purposes of this study, a parametric analysis of the interrelationship between the thermal state of the components and the parameters of the combustion cycle involved, using the analytical descriptions of the first group's α_{gas}, was developed based on the similarity theory; these include the main design parameters of the engine under study, the chemical properties of the working body, and the thermodynamic parameters characterizing the operating loads of the engines.

2. Methodological Aspects: Selection and Justification of the Analytical Form of α_{gas} Calculation

According to the set goal in the publication, the methodological aspects became the main issues to be addressed. Therefore, the second methodological section is dedicated to identifying and justifying one of the most rational parameter structures determining the heat exchange intensity for practical use. Based on the solutions presented in the second section, the third section develops solutions for the created methodology, describes the algorithms and their implementation using IT tools, and provides an application example.

Most of the solutions for using simplified α_{gas} models have been extensively validated on different types of ICEs operating over a wide load range and on different fuels. In particular, the model proposed by Woschni et al. [21] is commonly used to solve practical problems. Further, the analytical solution in [21] has been widely used in single-zone combustion cycle models such as AVL BOOST [28,30]. Woschni et al. and Merker et al. [21,33] made the theoretical assumption of a stationary, fully turbulent tube flow. Their formulae were based on the similarity theory criteria, which describe the intensity of heat release (Nu), the intensity of fluid flow around the parts (Re), and the physical and chemical properties of fluids (Pr). Furthermore, they distinguished the peculiarities of using this formula for different strokes and validated it for various engine models. For the dimensionless heat transfer coefficient Nu, a semi-empirical equation was obtained from a dimension analysis, as follows, essentially filling the structure with the characteristic parameters of ICEs:

$$Nu = C*Re^{0.8}*Pr^{0.4}, \quad (2)$$

were Nu = $\frac{\alpha D}{\lambda}$, with λ denoting the thermal conductivity coefficient, α denoting the heat transfer coefficient, and D denoting the cylinder diameter; Re = $\frac{\rho w D}{\eta}$, with ρ denoting the density, η denoting the dynamic viscosity, and w denoting the speed, assumed to be the average piston speed; and Pr = $\frac{\eta}{\rho}\alpha$.

For practical use, (2) was simplified to parameters that can be easily determined in a single-zone combustion model, thus allowing the heat transfer coefficient of the combustion cycle to be determined as follows:

$$\alpha_{gas} = 127.93 * D^{-0.2} * \rho^{0.8} * w^{0.8} * T^{-0.53}, \text{ W}/(\text{m}^2\text{K}) \quad (3)$$

Similarly, widely validated analytical solutions based on Equation (4) have been performed at the Central Diesel Engine Research Institute (CDERI), St Petersburg, by Molodtsov et al. [34]. As experimentally determined in [34,35], the heat transfer coefficient α_{gas} and CPG temperature depend primarily on the cylinder diameter, the average piston speed, the composition of the working body, the pressure, and the temperature. The structural equation proposed in [34] describes the variation character of the heat transfer coefficient from the listed parameters.

$$\alpha_{gas} = A * P_r^{0.4} * \frac{\lambda_{p\ gas}}{\mu_{gas}^{m}} * \frac{C_m^m}{D^{1-m}} * \left(\frac{P_{gas}10^4}{R_{gas}\ g\ T_{gas}}\right)^m, \text{ W}/\left(\text{m}^2\text{K}\right) \quad (4)$$

The first part of the above equation, A $P_r^{0.4}\frac{\lambda_{gas}}{\mu_{gas}^m}$, reveals the gas composition and the influence of the parameters, where A = 2.75 + 58.6 (D/c_m), according to the static generalization of the parameters, and c_m is the average piston velocity. The second part, $\frac{C_m^m}{D^{1-m}}$, describes the dependence of α_{gas} on the main engine design parameters and operating mode. The third part, $\left(\frac{P_{gas}10^4}{R_{gas}\ g\ T_{gas}}\right)^m$, represents the thermodynamic parameters of the combustion cycle of the working process. Thus:

$$\alpha_{gas} = \left(2.75 + 58.6\frac{D}{C_m}\right) * \frac{\lambda_{p\ gas}}{\mu_{gas}^{0.5}} * \left(\frac{C_m}{D}\right)^{0.5} * \left(\frac{P_{gas}10^4}{R_{gas}\ g\ T_{gas}}\right)^{0.5}, \text{ W}/\left(\text{m}^2\text{K}\right) \quad (5)$$

where α_{gas} is the current heat transfer coefficient during the cycle; $\lambda_{p\ gas}$ is the gas heat conductivity coefficient (W/(m K)); μ_{gas} is the gas viscosity coefficient (kg/(m·s)); P_{gas} and T_{gas} are the current gas pressure (N/m^2) and temperature (K) during the cycle, respectively); c_m is the average piston velocity (m/s); D is the cylinder diameter (m); R_{gas} is the gas constant (J/(kg·K)); and g is the free-fall acceleration.

In determining the numerical values of the constants, A and m, generalized test data from a wide range of high-speed and medium-speed diesel engines with volumetric mixture formation, both turbocharged and naturally aspirated, were utilized: 12/14, H18/22, 25/34, and 26/26. The experience of the successful application of this equation in investigating the thermomechanical state of components in the cylinder–piston group of engines such as 15/15, 15/18, 16.5/18.5, and 16.5/15.5 was also considered [36].

Thus, the α_{gas} calculations by Woschni et al. and CDERI are typically used to calculate each crankshaft rotation angle. However, the CDERI model has also been adapted for parallel generalized use in an integral form when $\alpha_{gas\ av}$ is calculated for the entire heat exchange cycle α_{gas} = (φ). This feature is significantly advantageous, particularly in the Klaipeda University studies, during which the combustion cycle parameters, which determine the energy efficiency, are optimized. These parameters are also evaluated in the integral form of the entire combustion cycle. The proposed methodological solution using $\alpha_{gas\ av}$ has been successfully validated in the research and design of ICE models tuned for various average pressures [33,34]. Based on these fundamentals, $\alpha_{gas\ av}$ [34,35] was used to form an interrelated combustion cycle algorithm.

3. Results of Research: Parametric Analysis of Combustion Cycle Indicators and Thermal Load

The relationship among the average heat transfer coefficient $\alpha_{gas\ av}$, the average temperature of the entire engine working cycle $T_{gas\ av}$, and the combustion cycle parameters is based on a mathematical engine combustion cycle model. Here, note that $\alpha^{com}_{gas\ av\ T}$ and $T^{com}_{gas\ av\ T}$ denote the average heat transfer coefficient and the average temperature for the part of the cycle section when heat is transferred to the component, respectively. The use of a single-zone MM enables the calculation of the current values of the parameters of the working body and the characteristics of heat release during the cycle, along with the characteristic parameters of the combustion cycle T_{gas}, P_{gas}, X = f(λ, ε, λ_p, P_k, T_k), where ε is the compression ratio and λ_p is the degree of pressure increase. Thus, the dependence of the heat transfer coefficient [34,35] can be simplified when applying it to a specific engine model for transferring it to LCFs, as follows:

$$\alpha_{gasav} = \left(2.75 + 58.6\frac{D}{C_m}\right) * \frac{\lambda_{p\ gas}}{\mu_{gas}^{0.5}} * \left(\frac{C_m}{D}\right)^{0.5} * \left(\frac{P_{gas}}{R_{gas}T_{gas}}\right)^{0.5},\ W/\left(m^2K\right) \tag{6}$$

For structurally similar engines at a constant working speed (c_m), the multipliers $\left(2.75 + 58.6\frac{D}{C_m}\right)\left(\frac{C_m}{D}\right)^{0.5}$ can be converted to a constant (N):

$$\alpha_{gas\ av} = N * \frac{\lambda_{p\ gas}}{\mu_{gas}^{0.5}} * \left(\frac{P_{gas}}{R_{gas}T_{gas}}\right)^{0.5},\ W/\left(m^2K\right) \tag{7}$$

The universality of the formula, when applied to both petroleum-derived fuel and the use of low-carbon fuels (LCFs), is related to the existing structural parameters $\lambda_{p\ gas}$ and μ_{gas} (corresponding to the conductivity and the viscosity of the combustion products in the engine cylinder, respectively), which differ for various fuel types. The peculiarities of the LCF combustion cycle also result in different values of the parameter X, which influences both $\lambda_{p\ gas}$ and the engine's modeled energy indicators. This structural connection is revealed by a system of Equation (8).

The transition to an interrelated parametric analysis with combustion cycle parameters is represented by the following system of equations:

$$\begin{cases} T_{gas},\ P_{gas},\ X = f(\lambda, \varepsilon, \lambda_p,\ P_k, T_k) \\ \lambda_{p\ gas},\ \mu_{gas} = f(\lambda, X, T_{gas}) \\ \alpha_{gas\ av} = N * \frac{\lambda_{p\ gas}}{\mu_{gas}^{0.5}} * \left(\frac{P_{gas}}{R_{gas}T_{gas}}\right) \end{cases} \tag{8}$$

The first Equation in (8) shows the influence of the characteristic indicators of the combustion cycle on the thermodynamic parameters of the cycle and the heat release characteristics; the second equation shows the formation of the physical properties of the working body; and the third equation is based on the first two equations.

The combined solution of these equations allows us to express the dependence of the similarity conditions of the heat transfer parameters from the working body to the component, as follows (P_{max}-fixed):

$$\alpha_{gas\ av}, T_{gas\ av}\left(\alpha^{com}_{gas\ av\ T}, T^{com}_{gas\ av\ T}\right) = f\left(\lambda, \varepsilon, \lambda_{p\ gas}, \mu_{gas}, P_k, T_k\right) \tag{9}$$

The transition to the average of the heat exchange process is $\alpha^{com}_{gas\ av\ T}$, $T^{com}_{gas\ av\ T}$. The alternative solution is implemented in two ways: the first one is based on the analysis of statistical multivariate data [36,37], where significant factors are identified and separated using the influencing factor. This enables an assessment of the thermal load level on the components for various combustion cycle organization strategies and the selection of the most rational one when optimizing energy and environmental performance. For practical applications, the dependencies of $\alpha^{com}_{gas\ av\ T}$, $T^{com}_{gas\ av\ T}$ are presented as a function of the interrelated parameters of the diesel engine, i.e., P_{max}/P_k, λ, ε, λ_p, and T_k, and the methodological approach can be applied for choosing the most rational combination. The influence of the charge air parameters on cylinder filling is reflected by additional factors. Thus, the conditions to perform a simultaneous parametric analysis between the characteristics of the combustion cycle process and the thermal and mechanical stress of the piston group from the function of the values P_{max}/P_k, λ, and ε or ε, λ, λ_p, P_k, and T_k with respect to $P_{max}/P_k = \varepsilon^{\ n}\ \lambda_{\ p}$ are met.

The second is based on modeling the combustion cycle of a specific engine model or an "engine family", preferably using a single-zone mathematical model. In this process, the heat transfer coefficients to the walls from the working fluid of the engine components are calculated, and based on these coefficients, the heat losses to the cooling system are determined. The choice of methods is determined by the research tasks and the availability of necessary parameters for calculating $\alpha_{gas\ av}$ and $T_{gas\ av}$ for the studied object. However, in both cases, an assessment of the adequacy of the obtained heat exchange parameters for practical use can be performed by comparing them with the engine's thermal balance data.

For greater clarity, a block diagram of the combined parametric analysis model is presented in Figure 1. The implemented algorithm serves as the foundation for addressing the planned research tasks aimed at expanding the use of LCFs in the main and auxiliary engines of operational vessels.

The features of the method allow for an interrelated parametric analysis. The method is adaptive for a wide range of engine loads based on the average indicator (effective) pressure p_{mi} (p_{me}). This is relevant to the practical application of the method in the context of different in-service engine models of the same engine type and addresses the challenge of using LCFs in the study of engines within a so-called "family", the models of which differ in their level of boost, configuration of the main systems, and structure of the operating loading cycle on the vessel.

The combinations of the sets λ, ε, λ_p, P_k, and T_k can be identified to calculate $\alpha^{com}_{gas\ av\ T}$ and $T^{com}_{gas\ av\ T}$ and plot the resulting values on a graph in parallel with the energy efficiency (η_i). As the ε, λ, P_k, and T_k values are available for optimization for the chosen simple retrofitting, further studies will be conducted by changing ε and recalculating $\alpha^{com}_{gas\ av\ T}$ and $T^{com}_{gas\ av\ T}$ for all of the selected operating parameters. The aim is to simulate the duty cycle process for an engine running on LCFs with similar effective power indicators p_{me} as an engine running on fossil fuel, with a maximum achievable η_i. The LCFs (line shape) combination of $\alpha^{com}_{gas\ av\ T}$ and $T^{com}_{gas\ av\ T}$ in the graph must not exceed the calculated thermal stresses of the engine running on fossil fuel. Studies based on a similar methodology and the set goals of boosting engines and justifying the design solutions for parts have been conducted [37,38]. The reliability of various engine structural components was investigated for promising model types by increasing the average indicator pressure p_{mi}.

In this context, there are practically no differences in the implementation of the successfully tested combined analysis method, both in terms of the tasks related to diesel engine boosting and in the planned retrofitting of operational models within a certain power range of a family of diesel engines. Below is a proposed example of implementing such an approach. For the studied models of the "family" of operational engines in the characteristic power range of p_{mi} = 1.2, 1.4, and 1.6 MPa, the possible retrofitting options for organizing the combustion cycle combinations of λ, P_k, λp, and ε (four combinations for the fixed levels of λ = 1.75, 2.0, 2.25, and 2.5) are determined within the technological accessibility constraints. This is achieved with limitations on P_{max} and a selected variant of the supercharged air-cooling system under the condition T_K = const. The maximum P_{max} should be set based on the real strength reserves of the components of the cylinder–piston group (CPG) and the crankshaft mechanism (CM) of the "family" models declared by the manufacturer for operation on diesel fuel.

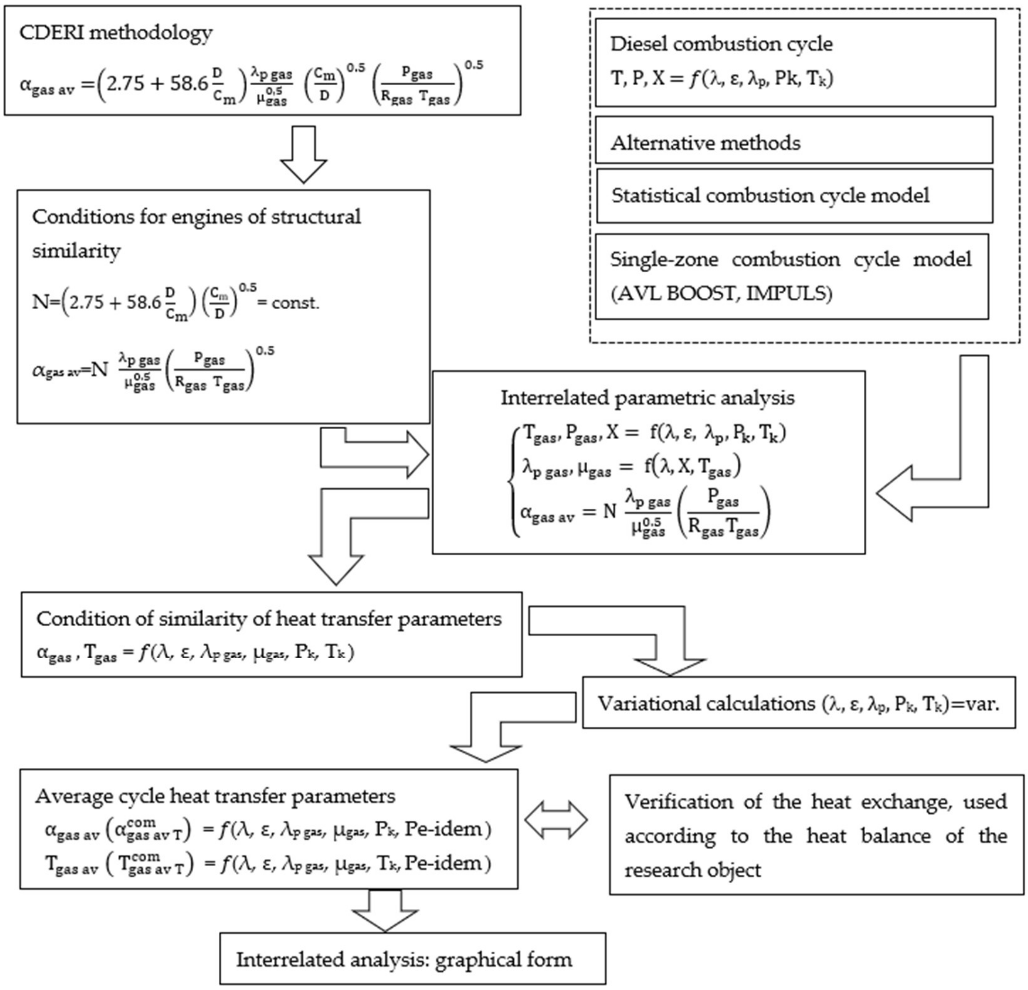

Figure 1. Block diagram of the combined parametric analysis model.

Due to technical allowances in the manufacturing of components and the regulation of diesel assemblies, the value of P_{max} for the same models of a "family" of diesel engines varies within a specific range. Typically, its magnitude does not exceed ±2–3% of the nominal value of P_{max} that is regulated by technical documentation. This circumstance is assumed to be taken into account when performing a parametric analysis of the indicator process using the developed algorithm. Its implementation includes the following sequence of operations:

1. For the analyzed power range of "family" models, p_{mi}, given the a priori values of P_{max} and T_k based on the specification or measurement on the vessel (in accordance with the mechanical strength reserves of the components of the cylinder–piston group and the chosen supercharged air-cooling system), ranges of rational changes in the defining parameters of the combustion cycle organization λ and ε are formed (specifically for the considered example, λ = 1.75, 2.0, 2.25, and 2.5).
2. Based on the theoretical relationship between diesel parameters for the identified values of λ, the initial data for determining the heat exchange indicators are calculated, relying on statistical data or combustion cycle modeling.

3. After determining the assessed levels of p_{mi}, combinations of λ, λ_p, ε, P_k, and T_k are calculated according to the methodology [38], providing the values of the average heat exchange parameters in the cylinder $\alpha^{com}_{gas\ av\ T}$ and $T^{com}_{gas\ av\ T}$.
4. The obtained combinations $\alpha^{com}_{gas\ av\ T}$ and $T^{com}_{gas\ av\ T}$ are plotted in the nomogram field $\alpha^{com}_{gas\ av\ T}$, $T^{com}_{gas\ av\ T}$ (see Figure 2). As a result, each of the analyzed levels of forcing by p_{mi} correspond to its own local area in the nomogram field, delimited by eight combinations of $\alpha^{com}_{gas\ av\ T}$ and $T^{com}_{gas\ av\ T}$. For the clarity and convenience of the subsequent analysis, lines of the fixed values of λ = 1.75, 2.0, 2.25, and 2.5 are displayed in the field of forcing areas (based on the possibility of increasing λ through a corresponding adjustment to the supercharging unit or its replacement).

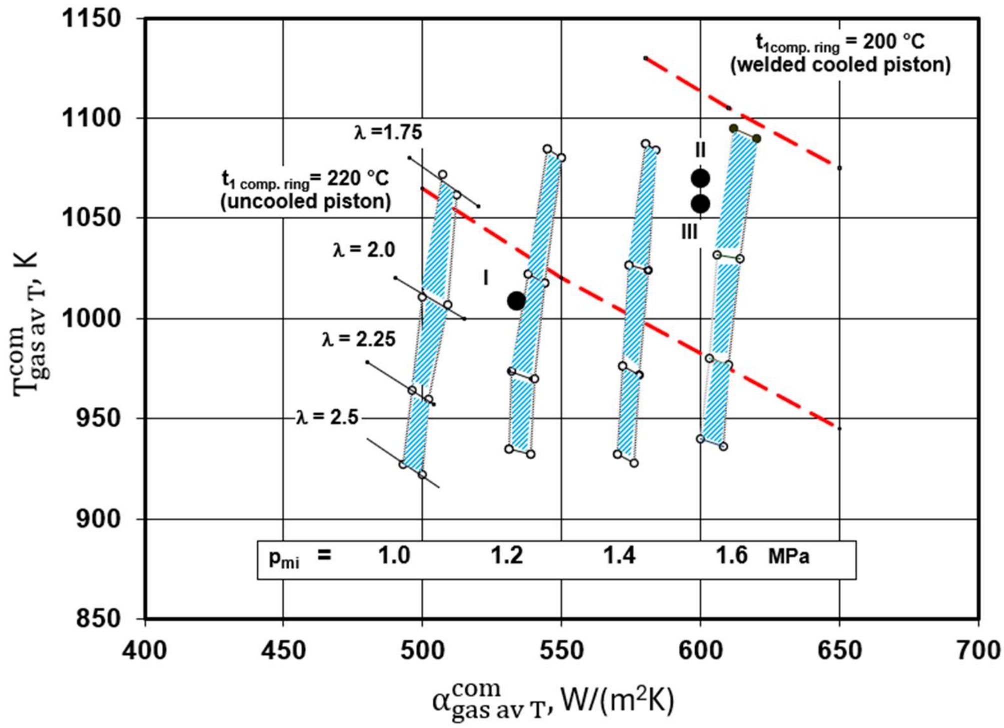

Figure 2. Fragment of an example illustrating combined parameters and thermal loads on the components of the cylinder–piston group of the 15/15 diesel "family" models during operation on the studied low-carbon fuel.

In terms of the fuel economy indicators, all of the considered combinations of λ, P_k, λ_p, and ε are invariant since, with a fixed p_{mi}, they fulfill the condition of a close fuel economy. To choose their rational combinations based on the thermal stress indicators, the indicators limiting the reliable operation of the examined model's piston when using diesel fuel (maximum surface temperature, temperature of characteristic zones of construction T_{com}, and stresses σ_{com}) were plotted on the nomogram in the form of isolines of constant values. The introduction of multiple criteria into the analysis allows the limiting factors to be determined and concentrates attention on them during the optimization of the indicator process parameters. In Figure 2, the reliability of the uncooled piston's operation is associated with the level of the characteristic temperature in the zone of the first compression ring: its maximum value when using oils with additives and considering operational conditions is accepted as $t_{1comp\cdot ring}$ = 220 °C.

It is important to note that the developed approach is not limited to the framework of a quasi-stationary piston-loading analysis. Evaluations of piston construction that consider the fatigue strength reserves for the total stresses arising from the action of the stationary temperature field and variable loads from the impact of P_{max} are possible. In this case, it is rational to use the results of the piston fatigue tests, generalized in the form of a

Goodman–Soderberg diagram, as exemplified by the company Wellworthy Piston Rings Limited and in the materials of several other studies.

The analysis of the mutual position of the isolines T_{com}, σ_{com} = const. with the fields of investigated forcing levels by p_{mi} allows for a multivariate assessment of the rational organization of the combustion cycle when transitioning the operation of the examined engine "family" models to a wide range of LCFs. Figure 2 provides an example of using the developed algorithm for the combined parametric analysis method for the "family" of 15/15 models.

The Roman numerals I and II (III) correspond to the level of forcing of two models of the "family", p_{mi} = 0.95 MPa and p_{mi} = 1.17 MPa, respectively. With an equal thermal piston load, the reserve of applying LCFs for the "family" models in the characteristic power range p_{mi}, compared to the diesel fuel baseline, is approximately 20%: 1.4 MPa versus 1.15 MPa. Evidence of this is also provided by the position of the point corresponding to p_{mi} = 0.95 MPa for the standard configuration of the diesel in the field of prospective forcing at p_{mi} = 1.2 MPa. The predominant influence on the temperature state of the piston assembly is exerted by λ. Theoretically, its increase from 1.75 to 2.25 (due to the readjustment of the turbocharger or its replacement during retrofitting) allows a nearly constant heat load to be maintained on the piston in the investigated p_{mi} range and limits the use to the uncooled piston modification. Under real conditions, ensuring reliable starting characteristics of diesel engines of this size restricts the boundaries of the possible reduction in ε to the level of 13–14 units. Accordingly, the range of possible changes in λ narrows, as otherwise, considering the low dynamics of the indicator process, the condition for limiting P_{max} would not be met. As a result, the theoretical transition to an oil-cooled piston design, in case of its technological implementation with the accepted position of the thermal stress limit line $t1_{comp \cdot ring}$ = 220 °C on the nomogram and the implementation of λ = 2.0, becomes necessary for "family" models with a p_{mi} > 1.2 MPa.

Thus, the provided example of using the applied method illustrates the principle of influencing the magnitude of the thermal load with the aim of fully utilizing the potential of different models within the operated diesel family for transitioning their operation to LCFs.

One of the key conditions for the effective use of the developed parametric analysis is the justified assignment of the restrictive levels $\alpha^{com}_{gas\ av\ T}$ and $T^{com}_{gas\ av\ T}$ in the nomogram field (Figure 2). In contrast to the possibilities of research under laboratory conditions and at engine manufacturers, direct measurements of the temperature and stress of parts are not possible for operating models. In this case, a comparison of the data obtained will be used when the engine is running on base-oil fuel, for which the manufacturer guarantees certain reliability indicators (lifetime before overhaul, failure rates, etc.), and LCFs. This means that, after verifying the mathematical model of the object under study on the basis of a specification or experimental data, modeling the indicators and parameters of the heat exchange cycle of the traditional diesel fuel combustion cycle will be carried out. The resulting boundary isolines of the combinations after they are plotted in the parametric analysis nomogram field are supplemented by the results of similar calculations of LCF combustion cycle indicators in the form of local combinations of $\alpha^{com}_{gas\ av\ T}$ and $T^{com}_{gas\ av\ T}$. Based on a comparative analysis of the data obtained, it will be possible to make decisions about the possible optimization of combustion cycle indicators. At this stage, a statistical analysis of literary sources and our own research findings will be used [39–41].

Possible uncertainty in the results of the parametric analysis is associated with the use of dependencies ($\alpha^{com}_{gas\ av\ T}$) for cases where LCFs are used, although the authors of a number of analytical dependencies declare their use for many types of fuels [42,43]. However, the research algorithm also provides for the possibility of adjusting the structure of the calculated λ dependencies, primarily the multiplier constants, based on the comparison of the experimental and calculated items of the engine heat balance [43], as tested by the authors. The predicted accuracy of the methodology hinges on the practical application of its results, evaluating the range limits of diesel engine boosting by increasing the p_{me} (p_{mi}) [36]. The use of the α formula, widely validated for diesel fuel, ensured that the methodology's error did not surpass 2–3%. In the case of LCF usage, addressing the uncertainty arising from the applicability of the α formula involves verifying the formula based on engine heat balance data [43], resulting in an estimated error of 2–4%.

Based on previous authors' research on the four-stroke, four-cylinder diesel engine 79.5/95.5 running on diesel and dual Diesel/NG fuel, a proposed methodological use case fragment can be provided. When the engine operates on diesel fuel with a specified injection angle of 1 crank angle degrees (CAD) before top dead center (TDC), the energy efficiency index η_e reaches 0.365 at a load of p_{me} = 8 bar (2000 rpm). However, when switching the engine to dual fuel D20/NG80 (with the maximum experimentally achieved NG ratio), the η_e drops by 9–45% across the entire tested load range from 2 bar to 8 bar. Consequently, fuel overdraft exacerbates the reduction in harmful emissions due to the NG effect (NG forced into the cylinder during low-pressure intake strokes along with the air). To enhance engine efficiency (η_e) and ecological indicators without significant modernization, the pilot diesel injection timing was advanced to 13 degrees CAD before TDC. This resulted in a significantly smaller decline in energy efficiency compared to diesel, down to 19–5%, while notably enhancing ecological indicators (in all instances, the mechanical engine components' load factor P_{max} did not surpass the specified limits). The results of the thermal load assessment of the engine components temperature of the first compression ring zone are presented in Figure 3. The thermal load restriction of the piston is conditionally accepted based on p_{me} = 8 bar when operating on diesel (considering that experimental and computational studies of the piston's temperature field have not been conducted). When the engine operates on D20/NG80 with a specific injection angle of φ_{inj} = 1 CAD before TDC (blue line), the piston thermal load $\alpha^{com}_{gas\ av\ T}$ and $T^{com}_{gas\ av\ T}$ form does not exceed the set limit (dashed line). It is worth noting that according to G. Woshni's methodology, α_{gas} results were refined based on engine heat balance data. However, increasing φ_{inj} to 13 CAD before TDC ($\alpha^{com}_{gas\ av\ T}$, $T^{com}_{gas\ av\ T}$) already exceeds the allowable limits at p_{me} ~7, bar. The main reason is the significant increase in characteristic $T_{gas\ av}$ temperature. Based on this, one rational measure could be to increase the air–fuel equivalence ratio λ. The results of evaluating the obtained effect can also be rationally represented in the form of $\alpha^{com}_{gas\ av\ T}$, $T^{com}_{gas\ av\ T}$ diagrams. Decarbonization indicators in the maritime sector are declared in accordance with a certain dynamic of fossil fuel substitution by LCF [1,2]. Therefore, among other decisions acceptable for real-world operation, is a change in the dual diesel/NG fuel composition, for example, reducing the NG portion to D40/NG60 (which was also experimentally investigated and shown in Figure 3, green curve). The adverse impact of the change in η_e and harmful emissions, when compared to diesel, was smaller and is similar to D20/NG80 at 13 CAD before TDC, and the piston heat load also does not exceed the specified limit.

However, in some cases, the use of a single-zone module alone may not effectively solve the optimization problems of engine parameters for operation on LCF. This may primarily be due to the lack of adapted analytical solutions for the investigated LCF.

As acknowledged, the accuracy of single-zone models relies heavily on precise heat release characteristic (HRC) data. Therefore, optimization solutions involve various technologies and combinations thereof, particularly changing the characteristics and delivery strategies into the LCF cylinder, among others. Significant changes also occur in the HRC simultaneously. Therefore, in cases where verified analytical solutions for a specific fuel type are lacking, it is reasonable to consider the possibility of additional application of a multi-zone model over a single-zone model. For the assessment of engine HRC while operating on LCF, multi-zone models are employed initially. Subsequently, the analytically derived and generalized HRC data obtained can be effectively incorporated into a single-zone model through extensive numerical investigations.

Moreover, ECU experimental indicator diagrams (controlled by ECU in modern medium- and low-speed ship engines) can also serve as a source of HRC determination. Furthermore, the selected α model (e.g., G. Woschni) is refined based on engine heat balance data.

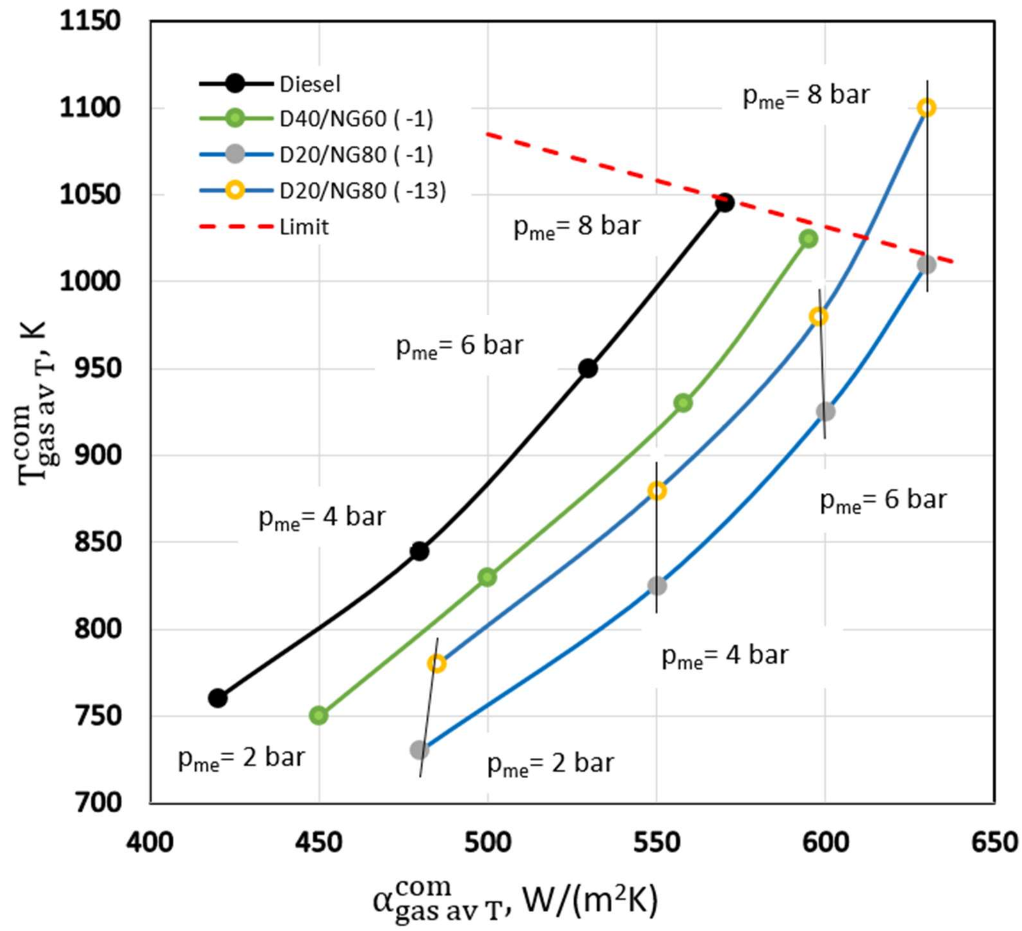

Figure 3. Engine (79.5/95.5) piston thermal load factor optimization fragment (n = 2000 rpm).

4. Conclusions

The presented methodological solutions addressing the decarbonization challenges in maritime transport aim to implement a comprehensive approach to enhance the performance of operational marine diesel engines when transitioning from fossil fuels to renewable and low-carbon alternatives. The proposed algorithm for a combined parametric analysis enables the assessment of an acceptable level of thermal load on the most stressed components of the cylinder–piston group. This assessment is conducted while optimizing the combustion cycle parameters for LCFs to improve the energy efficiency and reduce the emissions of toxic and greenhouse gases.

The implementation of a combined analysis of the heat exchange parameters in the cylinder and the combustion cycle is based on the use of well-established α-formulae for heat exchange intensity (CDERI, G. Woschni). Alternatively, the modeling of the engine's combustion cycle involves the application of a statistical model developed by the authors, oriented towards identifying the factors influencing the thermal load in different combustion cycle organizations. It also includes known single-zone models such as AVL BOOST and IMPULS. In the latter case, the tasks of identifying the permissible power ranges for the "family" for LCF operation are solved.

The graphical environment for visualizing the obtained results is considered sufficiently versatile for conducting comprehensive research, as it is not limited to a specific optimization strategy for combustion cycle parameters. The authors associate the long-term goal of the obtained results with the application of methodological solutions for a parametric analysis in ongoing studies on the use of ammonia in medium-speed marine diesel engines.

Author Contributions: Conceptualization, S.L. and E.M.; methodology, S.L.; writing—original draft preparation, E.M.; visualization, E.M.; supervision, S.L. All authors have read and agreed to the published version of the manuscript.

Funding: The project was financed by Research Council of Lithuania and the Ministry of Education, Science and Sport Lithuania (Contract No. S-A-UEI-23-9).

Institutional Review Board Statement: Not applicable.

Informed Consent Statement: Not applicable.

Data Availability Statement: No new data were created in this study. Data sharing is not applicable to this article.

Acknowledgments: The authors would like to thank the Klaipeda University Faculty of Marine Technology and Natural Sciences for their support.

Conflicts of Interest: The authors declare no conflicts of interest.

Abbreviations

The following abbreviations are used in this manuscript:

LCF	low-carbon fuel
MM	mathematical model
GHG	greenhouse gas
IMO	International Maritime Organization
DNV	Det Norske Veritas
ICE	internal combustion engine
CPG	cylinder–piston group
CM	crankshaft mechanism
DF	dual fuel
CAD	crank angle degrees
TDC	top dead center
CDERI	Central Diesel Engine Research Institute, St. Petersburg

References

1. European Commission. COM(2021) 562 Final 2021/0210 (COD). 2021. Available online: https://opac.oireachtas.ie/Data/Library3/Documents%20Laid/2021/pdf/TRAdocslaid110821_110821_152830.pdf (accessed on 10 December 2023).
2. International Maritime Organization. Resolution MEPC.328(76). 2021. Available online: https://www.imo.org/en/OurWork/Environment/Pages/Index-of-MEPC-Resolutions-and-Guidelines-related-to-MARPOL-Annex-VI.aspx (accessed on 10 December 2023).
3. European Commission. COM(2021) 559 Final 2021/0223 (COD). 2021. Available online: https://eur-lex.europa.eu/resource.html?uri=cellar:dbb134db-e575-11eb-a1a5-01aa75ed71a1.0001.02/DOC_1&format=PDF (accessed on 10 December 2023).
4. The Marine Environmental Protection Committee. Resolution MERC.377(80). 2023. Available online: https://wwwcdn.imo.org/localresources/en/MediaCentre/PressBriefings/Documents/Resolution%20MEPC.377(80).pdf (accessed on 10 December 2023).
5. DNV. Achieving the IMO decarbonization Goals. Containership Insights. MARITIME IMPACT. 23 July 2020. Available online: https://www.dnv.com/expert-story/maritime-impact/How-newbuilds-can-comply-with-IMOs-2030-CO2-reduction-targets.html (accessed on 10 December 2023).
6. International Maritime Organization. Fourt IMO Greenhouse Gas Study. 2020. Available online: https://wwwcdn.imo.org/localresources/en/OurWork/Environment/Documents/Fourth%20IMO%20GHG%20Study%202020%20-%20Full%20report%20and%20annexes.pdf (accessed on 10 December 2023).
7. LR/UMAS. Techno Economic Assessment of Zero Carbon Fuels. 2020. Available online: https://www.lr.org/en/about-us/pressroom/press-release/lr-and-umas-publish-techno-economic-assessment-of-zero-carbon-fuels/ (accessed on 10 December 2023).
8. Solakivi, T.; Paimander, A.; Ojala, L. Cost competitiveness of alternative maritime fuels in the new regulatory framework. *Transp. Res. Part D Transp. Environ.* **2022**, *113*, 103500. [CrossRef]
9. MAN. Official Website. Available online: https://www.man-es.com/docs/default-source/document-sync/man-v51-60g-eng.pdf?sfvrsn=3776bc19_1 (accessed on 10 December 2023).
10. Yao, S.; Li, C.; Wei, Y. Design and optimization of a zero-carbon emission system integrated with the utilization of marine engine waste heat and LNG cold energy for LNG-powered ships. *Appl. Therm. Eng.* **2023**, *231*, 120976. [CrossRef]
11. Díaz-Secades, L.A.; González, R.; Rivera, N. Waste heat recovery from marine engines and their limiting factors: Bibliometric analysis and further systematic review. *Clean. Energy Syst.* **2023**, *6*, 100083. [CrossRef]

12. Chountalas, T.D.; Founti, M.; Tsalavoutas, I. Evaluation of biofuel effect on performance & emissions of a 2-stroke marine diesel engine using on-board measurements. *Energy* **2023**, *278*, 127845. [CrossRef]
13. Schroer, M.; Panagakos, G.; Barfod, M.B. An evidence-based assessment of IMO's short-term measures for decarbonizing container shipping. *J. Clean. Prod.* **2022**, *363*, 132441. [CrossRef]
14. Balcombe, P.; Staffell, I.; Kerdan, I.G.; Speirs, J.F.; Brandon, N.P.; Hawkes, A.D. How can LNG-fueled ships meet decarbonization targets? An environmental and economic analysis. *Energy* **2021**, *227*, 120462. [CrossRef]
15. Langari, J.; Aliakbari, K.; Nejad, R.M. Failure analysis of CK45 steel crankshaft in light truck diesel engine. *Eng. Fail. Anal.* **2023**, *145*, 107045. [CrossRef]
16. Venkatachalam, G.; Kumaravel, A. Experimental Investigations on the Failure of Diesel Engine Piston. *Mater. Today Proc.* **2019**, *16*, 1196–1203. [CrossRef]
17. Lu, Y.; Zhang, X.; Xiang, P.; Dong, D. Analysis of thermal temperature fields and thermal stress under steady temperature field of diesel engine piston. *Appl. Therm. Eng.* **2017**, *113*, 796–812. [CrossRef]
18. Cabuk, A.S. Experimental IoT study on fault detection and preventive apparatus using Node-RED ship's main engine cooling water pump motor. *Eng. Fail. Anal.* **2022**, *138*, 106310. [CrossRef]
19. Fatigati, F.; Di Bartolomeo, M.; Cipollone, R. Development and experimental assessment of a Low Speed Sliding Rotary Vane Pump for heavy duty engine cooling systems. *Appl. Energy* **2022**, *327*, 120126. [CrossRef]
20. Di Giovine, G.; Mariani, L.; Di Battista, D.; Cipollone, R.; Fremondi, F. Modeling and experimental validation of a triple-screw pump for internal combustion engine cooling. *Appl. Therm. Eng.* **2021**, *199*, 117550. [CrossRef]
21. Woschni, G. *A Universally Applicable Equation for the Instantaneous Heat Transfer Coefficient in the Internal Combustion Engine*; SAE Technical Paper; SAE International: Warrendale, PA, USA, 1967; p. 670931.
22. Hohenberg, G.F. *Advanced Approaches for Heat Transfer Calculations*; SAE Technical Paper; SAE International: Warrendale, PA, USA, 1979; p. 790825. [CrossRef]
23. Annand, W.J.D. Heat Transfer in the Cylinders of Reciprocating Internal Combustion Engines. *Proc. Inst. Mech. Eng.* **1963**, *177*, 973–996. [CrossRef]
24. Sitkei, G.; Ramanaiah, G. *A Rational Approach for Calculation of Heat Transfer in Diesel Engines*; SAE Technical Paper; SAE International: Warrendale, PA, USA, 1972; p. 720027. [CrossRef]
25. Chang, J.; Güralp, O.; Filipi, Z.; Assanis, D.; Kuo, T.W.; Najt, P.; Rask, R. New Heat Transfer Correlation for an HCCI Engine Derived from Measurements of Instantaneous Surface Heat Flux. *SAE Trans.* **2004**, *113*, 1576–1593. [CrossRef]
26. Wu, Y.Y.; Chen, B.C.; Hsieh, F.C.; Ke, C.T. Heat transfer model for small-scale spark-ignition engines. *Int. J. Heat Mass Transf.* **2009**, *52*, 1875–1886. [CrossRef]
27. Rabeti, M.; Ranjbar, A.A.; Jahanian, O.; Ardebili, S.M.S.; Solmaz, H. Investigation of important semi-empirical heat transfer models for a natural gas fueled HCCI engine. *Energy Rep.* **2021**, *7*, 8652–8666. [CrossRef]
28. Depcik, C.; Alam, S.S.; Madani, S.; Ahlgren, N.; McDaniel, E.; Burugupally, S.P.; Hobeck, J.D. Determination of a heat transfer correlation for small internal combustion engines. *Appl. Therm. Eng.* **2023**, *228*, 120524. [CrossRef]
29. Hassan, M.A.S.M.; Razlan, Z.M.; Bakar, S.A.; Rahman, A.A.; Rojan, M.A.; Wan, W.K.; Ibrahim, Z.; Ishak, A.A.; Ridzuan, M.J.M. Derivation and validation of heat transfer model for Spark-Ignition engine cylinder head. *Appl. Therm. Eng.* **2023**, *225*, 120240. [CrossRef]
30. Petrichenko, R.M. Convective heat transfer in piston machines. In *Mechanical Engineering*; Leningrad Shipbuilding Institute: Leningrad, Russia, 1979.
31. Asadi, A.; Zhang, Y.; Mohammadi, H.; Khorand, H.; Rui, Z.; Doranehgard, M.H.; Bozorg, M.V. Combustion and emission characteristics of biomass derived biofuel, premixed in a diesel engine: A CFD study. *Renew. Energy* **2019**, *138*, 79–89. [CrossRef]
32. Choi, M.; Song, J.; Park, S. Modeling of the fuel injection and combustion process in a CNG direct injection engine. *Fuel* **2016**, *179*, 168–178. [CrossRef]
33. Merker, G.P.; Schwarz, C.; Stiesch, G.; Otto, F. *Simulating Combustion—Simulation of Combustion and Pollutant Formation for Engine-Development*; Springer: Berlin/Heidelberg, Germany, 2006; pp. 148–155.
34. Molodtsov, N.I.; Sokolov, P.V.; Vlasov, Y.Y. The influence of structural regulation indicators and augmentation level on heat release coefficient of gases to the surface of CPG parts. *Leningr. CDERI Proc.* **1975**, *69*, 3–17.
35. Molodtsov, N.I.; Sokolov, P.V.; Chirin, M.L. Experimental installations, methods, and results of studies of thermal parameters of diesel engines. *Leningr. CDERI Proc.* **1975**, *69*, 33–54.
36. Lebedevas, S.; Matievskij, D.D.; Lebedeva, G. Formation of power ranges for the use of a design range of pistons on Ch15/15 diesel engines. *Ser. Mech. Eng.* **2004**, *2*, 121–127. Available online: http://vestnikmach.ru/catalog/powgen/hidden/352.html (accessed on 10 December 2023).
37. Lebedevas, S.; Lebedeva, G. Mathematical model of combined parametrical analysis of Indicator process and thermal loading on the diesel engine piston. *Transp. Vilnius Tech.* **2004**, *19*, 108–118. [CrossRef]
38. Lebedevas, S.; Lebedeva, G.; Pikūnas, A.; Spruogis, B. A simultaneous parametric analysis of the in-cylinder processes for diesel engines. *Int. J. Veh. Syst.* **2011**, *18*, 18–45. [CrossRef]
39. Lebedevas, S.; Raslavičius, L.; Rapalis, P. Simulation of microalgae oil spray characteristics for mechanical fuel injection and CRDI systems. *Biomass Conv. Bioref.* **2022**. [CrossRef]

40. Lebedevas, S.; Čepaitis, T. Parametric Analysis of the Combustion Cycle of a Diesel Engine for Operation on Natural Gas. *Sustainability* **2021**, *13*, 2773. [CrossRef]
41. Kavtavaradze, R. Mathematical model of the complex heat exchange—Convection and radiation in the combustion chamber of the diesel engine. *Tech. Mech.* **1989**, *10*, 175–177.
42. Woschni, G. *Internal Combustion Engines*, 2nd ed.; TU Miunhen: Munich, Germany, 1988; 303p.
43. Dauksys, V.; Lebedevas, S. Comparative research of the dual-fuel engine exergy balance. *Energetics Vilnius Lith. Acad. Sci.* **2019**, *65*, 113–121.